Fateixa, S., Schneider, J., Kumar, S. and Böhm, R. (2022) 3D Printed Polymer Nanocomposites Engineered With Graphene and Metallic Nanoparticles for Optical Detection of Water Pollutants. In: 20th European Conference on Composite Materials (ECCM20), Lausanne, Switzerland, 26-30 Jun 2022, (Accepted for Publication).

There may be differences between this version and the published version. You are advised to consult the publisher's version if you wish to cite from it.

https://eprints.gla.ac.uk/275346/

Deposited on: 20 July 2022

Enlighten – Research publications by members of the University of Glasgow
http://eprints.gla.ac.uk

3D PRINTED POLYMER NANOCOMPOSITES ENGINEERED WITH GRAPHENE AND METALLIC NANOPARTICLES FOR OPTICAL DETECTION OF WATER POLLUTANTS

Sara Fateixa,[a] Johannes Schneider,[b] S. Kumar,[b] Robert Böhm[c]

a: Department of Chemistry – CICECO Aveiro Institute of Materials, University of Aveiro, 3810-193, Aveiro, Portugal.
b: James Watt School of Engineering, University of Glasgow, Glasgow, G12 8LT, UK
c: HTWK Leipzig, Faculty of Engineering, PF 30 11 66, 04251 Leipzig, Germany

Abstract: *The development of novel low-cost materials capable of exhibiting high performance, sensitivity and reproducibility are highly desirable for environmental quality monitoring of emerging chemical pollutants (ECPs). Their presence in water can be harmful and have unpredictable consequences for the environment and human health. Therefore, monitoring such ECPs is critical to improving water quality and preventing the increased incidence of several diseases. Here, we explore the performance of 3D printed polymer nanocomposites comprising graphene and gold nanoparticles (AuNPs) to detect ECPs in water using surface-enhanced Raman scattering (SERS). Fused filament fabrication additive manufacturing will fabricate samples using nanoengineered filaments comprising graphene and AuNPs. Nanoengineered filaments are prepared by melt blending using a twin-screw extruder. The composites' capability to detect the ECPs is evaluated using conventional and portable Raman instruments. Imaging techniques, namely confocal Raman microscopy, are used to optimize the Raman signal of the ECPs on the substrates.*

Keywords: 3D printed polymer nanocomposites; graphene; SERS; emerging pollutants.

1. Introduction

Emerging chemical pollutants (ECPs), also known as contaminants of emerging concern (CECs), are considered a severe problem worldwide. ECPs such as hormones, pharmaceuticals, pesticides and persistent organic pollutants are defined as new chemical compounds for which no regulation and monitoring protocols have been established yet. However, they can harm human health and the environment due to their persistence, resist biodegradation and bioaccumulation.[1,2] For example, antibiotics pose a significant concern because, even in vestigial amounts, they can cause health problems and contribute to antimicrobial resistance.[3,4] Typical analytical techniques such as high-performance liquid chromatography, capillary electrophoresis and liquid/gas chromatography-mass spectrometry have been used to detect vestigial amounts of ECPs.[5-7] However, these methods are time-consuming, cost-intensive and comprise complex laboratorial procedures. Therefore, novel technologies with high sensitivity, simple operations, in situ samplings, and portability are needed for detecting such environmental pollutants.

In this context, surface-enhanced Raman scattering (SERS) emerges as a promising method to monitor ECPs because it affords high sensitivity, spectroscopic fingerprints, easy sample preparation, and non-destructive analyses.[8-10] SERS is a vibrational spectroscopic technique for detecting molecules adsorbed on metal surfaces, typically Ag and Au.[11,12] Great progress was made to assemble such metals into nanostructures that act as stable, reproducible and

 ©2022 1st Author et al. https://doi.org/ 10.5075/978-X-XXX-XXXXX-X published under CC BY-NC 4.0 license

active SERS substrates to detect trace levels of molecules of interest.[13,14] These strategies envisage metal surfaces where an enhanced local electromagnetic field (hotspots) is observed. Hotspots have been proposed to occur in nanojunctions between closely spaced metallic nanoparticles (MNPs) by inducing colloidal aggregation in apexes of anisotropic nanostructures or decorating graphene sheets.[15-17] These hotspots originate highly enhanced local electromagnetic fields that allow Raman detection at the single-molecule level.[15,18,19] This makes SERS a valuable tool in the environmental detection of trace levels of ECPs, provided effective SERS substrates are available. Fateixa *et al*. have investigated a variety of hybrid structures for the optical detection of ECPs, including magnetic substrates,[20,21] inkjet printing paper-based platforms[22] and MNPs dispersed in a polymer matrix[23] or filter mambranes[24].

Fabricating highly sensitive, reproducible, stable, and cost-effective SERS templates remains an actively researched topic.[25-27] 3D SERS templates have recently gained particular interest due to their larger surface area, increasing the molecules uptake and, therefore, its detection.[28-31] By increasing the hotspots' number in the z-direction, the Raman signal of the ECP can be improved, and detection limits can be lowered.

Additive manufacturing (AM), also known as 3D-printing, has recently established itself as a technology that enables the production of new designs and materials and does not require expensive molds or tools, which makes it particularly valuable for prototyping, mass customizations, waste minimization and low processing costs.[32,33] Fused filament fabrication (FFF) is one of the most used and affordable 3D printing techniques, an extrusion-based process that enables layer-by-layer deposition of the thermoplastic polymers in x-y, and z direction to fabricate complex 3D structures. The filament feedstock can be tailored to improve materials properties such as stiffness, strength, and energy absorbing capabilities by adding micro- and/or nano-scale fillers, such as carbon fibers, carbon nanotubes or graphene nanoplatelets, which further can increase the materials electrical conductivity over several magnitudes and improve thermal conductivity, enabling new fields of application such as self-sensing devices for biomedical applications.[34-36] Carbon reinforced high performance composites are gradually replacing typical metallic materials due to their outstanding material properties and have excellent potential to significantly impact the manufacturing industry.[37]

Only one paper reports the fabrication of 3D-printed composites by FFF for SERS applications so far.[29] The authors have used 3D printing to fabricate highly sensitive reproducible SERS templates using a fluorenylmethyloxycarbonyl diphenylalanine hydrogel loaded with silver or gold NPs. The 3D-printed peptide-hydrogel composites were used to detect adenine molecules at concentrations as low as 100 pM. In this work, we use extrusion-based 3D printing method to fabricate 3D-SERS nanocomposites containing polylactic acid (PLA), graphene nanoplatelets (GNPs) and gold nanoparticles (AuNPs) as novel material technologies, envisaging their use for ECPs' extraction and detection in real complex water matrices (Figure 1). 3D-printed polymer composites are evaluated as SERS platforms for target antibiotics such as ciprofloxacin as a proof-of-concept for ECPs' monitoring. Confocal Raman microscopy is used to study the synergistic effect from the chemical mechanism between adsorbates on graphene-based materials and the local electromagnetic field formed by the AuNPs.

 ©2022 1st Author et al. https://doi.org/ 10.5075/978-X-XXX-XXXXX-X published under CC BY-NC 4.0 license

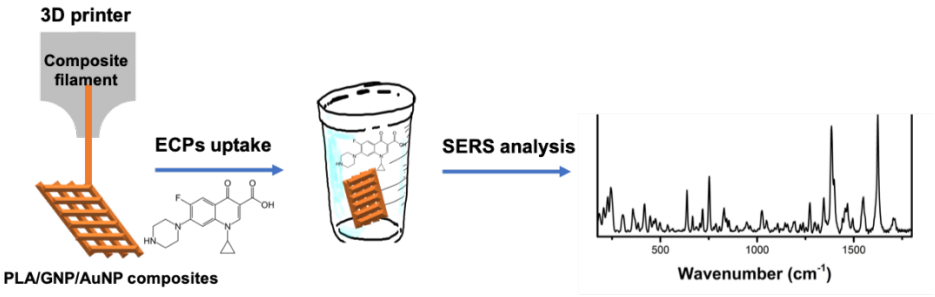

Figure 1. Preparation of PLA/GNP/AuNPs nanocomposites and the procedure for uptake and SERS detection of ECPs in water.

2. Experimental

2.1 Materials

The following chemicals were used as purchased: tetrachloroauric(III) acid trihydrate ($HAuCl_4 \cdot 3H_2O$, 99,9%, Sigma-Aldrich), ethylene glycol (EG, Aldrich, 99%), oleylamine (OA, Aldrich, 70%), Ciprofloxacin hydrochloride monohydrate (CIP, $C_{17}H_{18}FN_3O_3 \cdot HCl \cdot H_2O$, 99.0%, Sigma-Aldrich), Polylactic acid (4043D PLA pellets, Natureworks Ingeo), Graphene Nanoplatelets (2-10nm, ACS Material), Acetone (Sigma-Aldrich) .

2.2 Synthesis of organically capped-gold nanoparticles

Organically capped AuNPs were prepared using a modification of the polyol method described by Martins et al.[38] A solution containing $HAuCl_4 \cdot 3H_2O$ (0.15 M) in ethylene glycol (10 mL) was injected into a hot solution containing 40 mL of oleylamine (120 °C) for 30 min under a nitrogen stream. A dark red color solution is obtained after cooling to room temperature. The AuNPs were washed with 2-propanol and methanol and isolated by centrifugation (6000 rpm). The AuNPs were then dispersed in toluene.

2.3 Filament fabrication and 3D printing of PLA/Graphene blend and PLA/Graphene/AuNPs composites

The filaments are produced in-house with the Filabot EX6 extruder (Triex LLC dba Filabot), which has a three-stage extrusion screw made of hardened and polished stainless steel with a length-to-diameter ratio of 24:1. The feedstock is prepared by dry mixing PLA granules with the addition of GNPs and AuNPs, with the final mixing taking place in the extruder. Extruder temperatures are set at 167.5 °C, 166 °C, 165 °C and 40 °C for front, center, back and feed, respectively, using a 1.75 mm diameter die. To cool the extruded filament, it passes through the Filabot air path unit, using forced convection as it being extruded (fan speed 100%, Magnets: 5 used along airpath. end, center, front). The spool unit collects the filament and can be adjusted so that the filament diameter is precise within a range of 1.75±0.05 mm (settings used: drive–mid, traverse: 30%).

In this study, samples were fabricated using FFF technology, in which continuous thermoplastic filaments are fed from a spool through a heated nozzle, causing the material to melt and be deposited onto a heated print bed. The nozzle attached to the print head is able to move in-plane (x and y directions), while the print bed moves vertically (z direction), allowing the material to be applied layer by layer to form a final design. The 3D printer used is a Creator Pro (Zhejiang

 ©2022 1st Author et al. https://doi.org/ 10.5075/978-X-XXX-XXXXX-X published under CC BY-NC 4.0 license

Flashforge 3D Technology Co) with an extrusion temperature of 210 °C, a bed temperature of 60 °C, a layer height of 0.18 mm and an extrusion width of 0.48 mm (nozzle diameter 0.4 mm).

2.4 SERS studies

The sensitivity of 3D printing PLA/GNP/AuNPs composites was evaluated by SERS analysis coupled to Raman imaging. Raman images and spectra were acquired using a combined Raman-AFM-SNOM WITec alpha 300RAS+ microscopy. A Nd:YAG laser operating at 532 nm or a He:Ne laser operating at 633 nm were used as excitation sources.

Aqueous solutions of CIP with distinct concentrations (from 10^{-3} to 10^{-9} M) were prepared to establish the lower detection limit for the substrates used in SERS. The 3D printing PLA/GNP/AuNPs composites were placed in a vessel with the analyte solution to uptake the contaminant for several minutes (30min, 2h). Then, the composites were rinsed twice with distilled water to wash any unabsorbed analyte. The 3D printing PLA/GNP/AuNPs composites were transferred to a glass side and dried at room temperature before SERS analysis.

High-resolution Raman imaging was performed by taking 150 × 150 Raman spectra (in a total of 22500 spectra) in an area of 30 × 30 µm. A 100× objective was used to view samples, and the integration time for each spectrum was 0.05 s. Raman images were constructed by integrating the absolute area underneath the CIP Raman band at 1383 cm^{-1} (aromatic ring stretching) using WITec software (Project 5.0).

2.5 Instrumentation

TEM was carried out on a Hitachi H-9000 TEM microscope (Hitachi, Tokyo, Japan) operating at 300 kV. The TEM samples were prepared by placing a drop of the diluted AuNPs on a carbon-coated copper grid, and the solvent was left to evaporate in air. The 3D printing PLA/GNP/AuNPs composites were analyzed by scanning electron microscopy (SEM) using a SU-70 Hitachi instrument fitted with an energy- dispersive spectroscopy (EDS) accessory (EDS detector: Bruker AXS; software: Quantax), operated at 15 kV. Samples for SEM were placed on carbon tape and coated with carbon before the analysis in secondary electron (SE) and backscattered electron (BSE) modes. The XRD data were collected using a PAN analytical Empyrean X-ray diffractometer (PANanalytical, Almelo, The Netherlands) equipped with Cu K. The optical spectra were recorded using a GBC Cintra 303 UV/ VIS spectrophotometer. The spectra were recorded in diffuse reflectance mode using MgO as a reference for the 3D printing PLA/GNP/AuNPs composites. The corresponding absorption spectra were obtained by applying the Kubelka−Munk function to the experimental reflectance spectra.

3. Results

3.1 Characterization of the 3D printing of PLA/GNP/AuNPs composites

Organically capped Au NPs were prepared by reducing a gold salt in a mixture of long alkyl chain amines (e.g. oleylamine) and ethylene glycol. This reacting mixture promoted the formation of metal nuclei in a shorter period, resulting in AuNPs with an average size of around 25 nm. The TEM image of the AuNPs presents a spherical morphology of the particles with a significantly broader size distribution (Figure 2a). An average diameter of 24.7 ± 7.1 nm was obtained using the TEM image. The optical spectrum presented in Figure 2b shows an absorption band at 525 nm corresponding to the surface plasmon resonance (SPR) band characteristic for Au NPs.

 ©2022 1st Author et al. https://doi.org/ 10.5075/978-X-XXX-XXXXX-X published under CC BY-NC 4.0 license

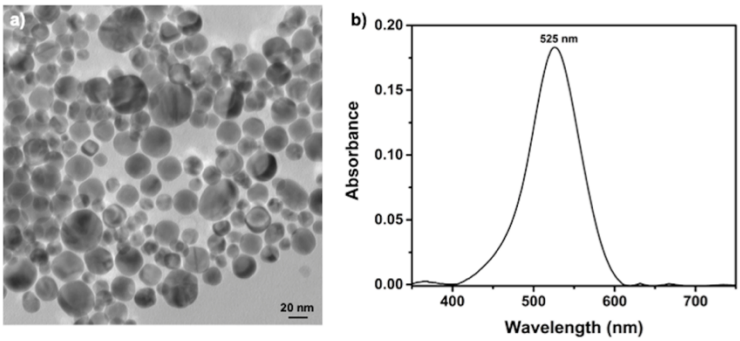

Figure 2. a) *Transmission electron microscopy (TEM) image of AuNPs and b) optical spectrum of organically capped Au NPs*

3.2 SERS studies

The as-prepared AuNPs were used as SERS substrates to detect CIP with a concentration of 10^{-5}M (pH 6). Figure 3A presents the SERS spectrum of CIP obtained using the AuNPs and the conventional Raman spectrum of CIP powder. It can be observed that the Raman spectrum of diluted CIP aqueous solution on the AuNPs is distinct from the pure solid analyte. The conventional Raman spectrum of CIP aqueous solution (10^{-5}M) did not present any Raman bands (data not shown). Therefore, the vibrational features observed in Figure 3Ab can only be explained by the SERS effect due to the presence of the AuNPs. The detection limit achieved for CIP using these AuNPs was lower as 10^{-7}M (Figure 3B).

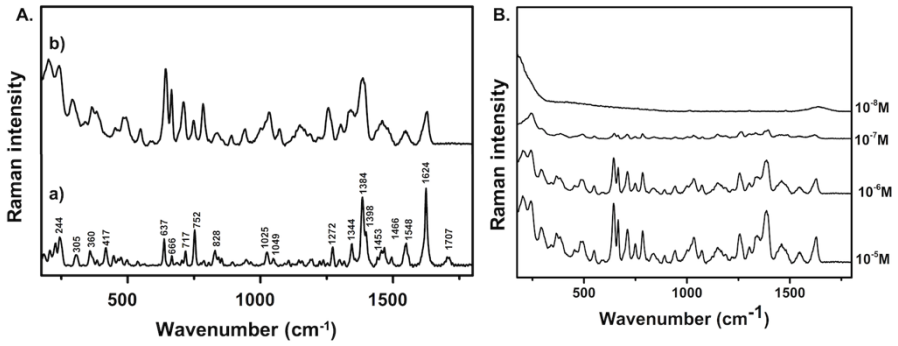

Figure 2. A. (a) Conventional Raman spectrum for CIP powder; (b) SERS spectrum of CIP aqueous solution (10^{-5} M) using the AuNPs; B. SERS spectra of CIP in distinct concentrations in AuNPs.

The incorporation of the AuNPs into graphene oxide sheets (Au/GO) can increase the CIP's Raman signal due to the synergistic effect between the graphene oxide (charge transfer) and AuNPs (enhancement of the electromagnetic field). The TEM image presented in Figure 4a shows bigger aggregates of AuNPs dispersed on the GO surface. These composites were used as nanosorbents to extract CIP from waters and analyzed by SERS imaging.

The Raman image shows the spatial distribution of CIP molecules (10^{-5}M) on the Au/GO surface (Figure 4b). The integration of the absolute area underneath the band at 1389 cm^{-1} (aromatic ring stretching) was used to establish the colour intensity and create the Raman image. Thus, the brighter colours in the image indicate regions with stronger SERS signal due to the presence of CIP molecules adsorbed in the AuNPs, simultaneously indicating the distribution of the AuNPs

 ©2022 1st Author et al. https://doi.org/ 10.5075/978-X-XXX-XXXXX-X published under CC BY-NC 4.0 license

over the GO sheets. The Raman image also shows that the AuNPs are evenly dispersed over the surface of the GO sheets, which agrees with the TEM results presented in Figure 4a.

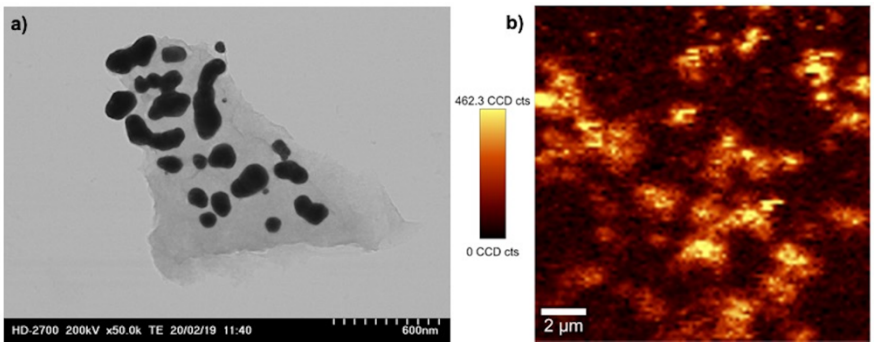

Figure 4. a) TEM image on Au/GO composite; b) Raman image obtained using the integrated intensity of the band at 1389 cm^{-1} in the SERS spectrum of CIP (10^{-5}M) using the Au/GO as substrates.

4. Conclusions

Preliminary results demonstrate that the AuNPs can be used as SERS substrates to detect CIP. The addition of AuNPs into the graphene-based materials results in highly stable composites with high sensitivity to extract and detect CIP from water. Further studies on 3D printing PLA/GNP/AuNPs composites must be performed to evaluate their sensitivity to uptake and detect CIP from water using SERS.

Acknowledgements

This work was developed within the scope of the project CICECO-Aveiro Institute of Materials, UIDB/50011/2020, UIDP/50011/2020 & LA/P/0006/2020, financed by national funds through the FCT/MEC (PIDDAC). S. F. thanks FCT for his research contract (REF-069-88-ARH-2018), which is funded by national funds (OE), through FCT-Fundação para a Ciência e a Tecnologia, I.P., in the scope of the framework contract foreseen in the numbers 4, 5, and 6 of the article 23, of the Decree-Law 57/2016, of August 29, changed by Law 57/2017, of July 19. The authors additionally acknowledge the support given by the European Commission via the COST Action CA19118 "High-performance carbon-based composites with smart properties for advanced sensing applications" (EsSENce). JS acknowledges EPSRC DTA PhD studentship [Award No: EP/R513222/1].

5. References

1. Lei M, Zhang L, Lei J, Zong L, Li J, Wu Z, Wang Z. Overview of emerging contaminants and associated human health effects. BioMed Res. Int. 2005; 2015:404796.
2. Tang Y, Yin M, Yang W, Li H, Zhong Y, Mo L, Liang Y, Ma X, Sun X. Emerging pollutants in water environment: Occurrence, monitoring, fate, and risk assessment. Water Environ. Res. 2019; 91:984.
3. Carvalho IT, Santos L. Antibiotics in the aquatic environments: A review of the European scenario. Environ. Int. 2016; 94:736.

 ©2022 1st Author et al. https://doi.org/ 10.5075/978-X-XXX-XXXXX-X published under CC BY-NC 4.0 license

4. Boxall ABA, Kolpin DW, Halling-Sørensen B, Tolls J. Are veterinary medicines causing environmental risks? Environ. Sci. Technol. 2003; 37:286A.
5. Petrie B, Youdan J, Barden R, Kasprzyk-Hordern B. Multi-residue analysis of 90 emerging contaminants in liquid and solid environmental matrices by ultra-high-performance liquid chromatography tandem mass spectrometry. J. Chromatogr. A 2016; 1431:64.
6. O'Sullivan-Carroll E, Howlett S, Pyne C, Downing P, Rafael A, Lynch M, Hogan AM, Moore EJ. Determination of Pharmaceuticals in Surface and Wastewater by Capillary Electrophoresis (CE): A Minireview. Anal. Lett. 2021; 55:1.
7. Gómez MJ, Gómez-Ramos MM, Agüera A, Mezcua M, Herrera S, Fernández-Alba AR. A new gas chromatography/mass spectrometry method for the simultaneous analysis of target and non-target organic contaminants in waters. J. Chromatogr. A 2009; 1216:4071.
8. Pinheiro PC, Daniel-da-Silva AL, Nogueira HIS, Trindade T. Functionalized Inorganic Nanoparticles for Magnetic Separation and SERS Detection of Water Pollutants. Eur. J. Inorg. Chem. 2018; 2018:3443.
9. Li DW, Zhai WL, Li YT, Long YT. Recent progress in surface enhanced Raman spectroscopy for the detection of environmental pollutants. Microchim. Acta 2014; 181:23.
10. Bodelón G, Pastoriza-Santos I. Recent Progress in Surface-Enhanced Raman Scattering for the Detection of Chemical Contaminants in Water. Front. Chem. 2020; 8:478.
11. Ding SY, Yi J, Li JF, Ren B, Wu DY, Panneerselvam R, Tian ZQ. Nanostructure-based plasmon-enhanced Raman spectroscopy for surface analysis of materials. Nature Rer. Mater. 2016; 1:1.
12. Langer J, *et al.* Present and Future of Surface-Enhanced Raman Scattering. ACS Nano 2020; 14:28.
13. Wang AX, Kong X. Review of recent progress of plasmonic materials and nano-structures for surface-enhanced raman scattering. Materials 2015; 8:3024.
14. Fateixa S, Nogueira HIS, Trindade T. Hybrid nanostructures for SERS: Materials development and chemical detection. Phys. Chem. Chem. Phys. 2015; 17:21046.
15. Chen T, Wang H, Chen G, Wang Y, Feng Y, Teo WS, Wu T, Chen H. Hotspot-induced transformation of surface-enhanced Raman scattering fingerprints. ACS Nano 2010; 4:3087.
16. Wei H, Xu H. Hot spots in different metal nanostructures for plasmon- enhanced Raman spectroscopy. Nanoscale 2013; 5:10794.
17. Zhu C, Zhao Q, Wang X, Li Z, Hu X. Ag-nanocubes/graphene-oxide/Au- nanoparticles composite film with highly dense plasmonic hotspots for surface- enhanced Raman scattering detection of pesticide. Microchem. J. 2021; 165:106090.
18. Mao, P, Liu C, Favraud G, Che Q, Han M, Fratalocchi A, Zhang S. Broadband single molecule SERS detection designed by warped optical spaces. Nat. Commun. 2018; 9:1.
19. Park WH, Kim ZH. Charge transfer enhancement in the SERS of a single molecule. Nano Lett. 2010; 10:4040.
20. Pinheiro PC, Fateixa S, Nogueira HIS, Trindade, T. Magnetite-supported gold nanostars for the uptake and SERS detection of tetracycline. Nanomaterials 2019; 2019:9.
21. Pinheiro PC, Fateixa S, Daniel-da-Silva AL, Trindade T. An integrated approach for trace detection of pollutants in water using polyelectrolyte functionalized magneto-plasmonic nanosorbents. Sci. Rep. 2019; 9:19647.
22. Martins NCT, Fateixa S, Fernandes T, Nogueira HIS, Trindade T. Inkjet Printing of Ag and Polystyrene Nanoparticle Emulsions for the One-Step Fabrication of Hydrophobic Paper-Based Surface-Enhanced Raman Scattering Substrates. ACS Appl. Nano Mater. 2021; 4:4484.

 ©2022 1st Author et al. https://doi.org/ 10.5075/978-X-XXX-XXXXX-X published under CC BY-NC 4.0 license

23. Fateixa S, Soares SF, Daniel-Da-Silva AL, Nogueira HIS, Trindade T. Silver-gelatine bionanocomposites for qualitative detection of a pesticide by SERS. Analyst 2015; 140:1693.
24. Fateixa S, Raposo M, Nogueira HIS, Trindade T. A general strategy to prepare SERS active filter membranes for extraction and detection of pesticides in water. Talanta 2018; 182:558.
25. Liu Y, Kim M, Cho SH, Jung YS. Vertically aligned nanostructures for a reliable and ultrasensitive SERS-active platform: Fabrication and engineering strategies. Nano Today 2021; 37:101063.
26. Mekonnen ML, Workie YA, Su WN, Hwang BJ. Plasmonic paper substrates for point-of-need applications: Recent developments and fabrication methods. Sensors Actuators B 2021; 345:130401.
27. Lee S, Choi, I. Fabrication Strategies of 3D Plasmonic Structures for SERS. Rev. Artic. BioChip. J. 2019; 13:30.
28. Almohammed S, Alruwaili M, Reynaud EG, Redmond G, Rice JH, Rodriguez BJ. 3D-Printed Peptide-Hydrogel Nanoparticle Composites for Surface-Enhanced Raman Spectroscopy Sensing. ACS Appl. Nano Mater. 2019; 2:5029.
29. Lee SY, Kim SH, Kim MP, Jeon HC, Kang H, Kim HJ, Kim BJ, Yang SM. Freestanding and Arrayed Nanoporous Microcylinders for Highly Active 3D SERS Substrate. Chem. Mater 2013; 25:2421.
30. Lee S, Hahm MG, Vajtai R, Hashim DP, Thurakitseree T, Chipara AC, Ajayan PM, Hafner JH. Utilizing 3D SERS active volumes in aligned carbon nanotube scaffold substrates. Adv. Mater. 2012; 24:5261.
31. García-Astrain C, Lenzi E, de Aberasturi DJ, Henriksen-Lacey M, Binelli MR, Liz-Marzán LM. 3D-Printed Biocompatible Scaffolds with Built-In Nanoplasmonic Sensors. Adv. Funct. Mater. 2020; 30: 2005407.
32. Schneider J, Kumar S. Multiscale characterization and constitutive parameters identification of polyamide (PA12) processed via selective laser sintering. Polym. Test. 2020; 86:106357.
33. Andrew JJ, Schneider J, Ubaid J, Velmurugan R, Gupta NK, Kumar S. Energy absorption characteristics of additively manufactured plate-lattices under low- velocity impact loading. Int. J. Impact Eng. 2021; 149:103768.
34. Arif MFF, Kumar S, Varadarajan KMK, Cantwell WJJ. Performance of biocompatible PEEK processed by fused deposition additive manufacturing. Mater. Des. 2018; 146:249.
35. Verma P, Ubaid J, Varadarajan KM, Wardle BL, Kumar S. Synthesis and Characterization of Carbon Nanotube-Doped Thermoplastic Nanocomposites for the Additive Manufacturing of Self-Sensing Piezoresistive Materials. ACS Appl. Mater. Interfaces 2022; 14:8361.
36. Andrew JJ, Alhashmi H, Schiffer A, Kumar S, Deshpande VS. Energy absorption and self-sensing performance of 3D printed CF/PEEK cellular composites. Mater. Des. 2021; 208:109863.
37. Koumoulos, E. P. *et al.* Research and Development in Carbon Fibers and Advanced High-Performance Composites Supply Chain in Europe: A Roadmap for Challenges and the Industrial Uptake. J. Composites Sci. 2019; 3:86.
38. Martins MA, Fateixa S, Girão AV, Pereira SS, Trindade T. Shaping gold nanocomposites with tunable optical properties. Langmuir 2010; 26:11407.

 ©2022 1st Author et al. https://doi.org/ 10.5075/978-X-XXX-XXXXX-X published under CC BY-NC 4.0 license